Encapsulation of small magnetic clusters in fullerene cages: A density functional theory investigation within van der Waals corrections

Polina Tereshchuk[1,*] and Juarez L. F. Da Silva[1,2,†]

[1]*Instituto de Física de São Carlos, Universidade de São Paulo, Caixa Postal 369, 13560-970 São Carlos, São Paulo, Brazil*

[2]*Instituto de Química de São Carlos, Universidade de São Paulo, Caixa Postal 780, 13560-970 São Carlos, São Paulo, Brazil*

(Received 30 November 2011; revised manuscript received 28 March 2012; published 29 May 2012)

The encapsulation of magnetic transition-metal (TM) clusters inside carbon cages (fullerenes, nanotubes) has been of great interest due to the wide range of applications, which spread from medical sensors in magnetic resonance imaging to photonic crystals. Several theoretical studies have been reported; however, our atomistic understanding of the physical properties of encapsulated magnetic TM $3d$ clusters is far from satisfactory. In this work, we will report general trends, derived from density functional theory within the generalized gradient approximation proposed by Perdew, Burke, and Ernzerhof (PBE), for the encapsulation properties of the $TM_m@C_n$ (TM = Fe, Co, Ni; $m = 2-6$, $n = 60,70,80,90$) systems. Furthermore, to understand the role of the van der Waals corrections to the physical properties, we employed the empirical Grimme's correction (PBE + D2). We found that both PBE and PBE + D2 functionals yield almost the same geometric parameters, magnetic and electronic properties, however, PBE + D2 strongly enhances the encapsulation energy. We found that the center of mass of the TM_m clusters is displaced towards the inside C_n surfaces, except for large TM_m clusters ($m = 5$ and 6). For few cases, e.g., Co_4 and Fe_4, the encapsulation changes the putative lowest-energy structure compared to the isolated TM_m clusters. We identified few physical parameters that play an important role in the sign and magnitude of the encapsulation energy, namely, cluster size, fullerene equatorial diameter, shape, curvature of the inside C_n surface, number of TM atoms that bind directly to the inside C_n surface, and the van der Waals correction. The total magnetic moment of encapsulated TM_m clusters decreases compared with the isolated TM_m clusters, which is expected due to the hybridization of the d-p states, and strongly depends on the size and shape of the fullerene cages.

DOI: 10.1103/PhysRevB.85.195461 PACS number(s): 74.20.Pq

I. INTRODUCTION

Transition-metal (TM) particles composed of a few (cluster) to 1000 (nanoparticle) atoms have been considered as potential candidates for a wide range of applications. For example, Rh, Pd, and Pt particles supported on oxides such as CeO_2 (Refs. 1 and 2) and Al_2O_3 are widely used in catalysis,[3,4] Au nanorods have been studied for selective release of drugs,[5] Rh nanoparticles (NPs) confined inside carbon nanotubes (CNTs) have been studied for ethanol production from syngas,[6] and Co NPs inside CNTs have been studied for tailoring the band gap of CNTs.[7] Furthermore, magnetic iron-oxide NPs and rare-earth atoms have been investigated as contrast agents for magnetic resonance imaging,[8,9] which is important for cancer therapy.

All those studies can be separated into three groups, namely, TM particles supported on oxides,[3,4] protected by ligands,[5] and encapsulated inside fullerenes and CNTs.[6,7] Thus, for real applications, clusters and NPs are in direct contact with an external environment, which can affect their atomic structure, relative stability, magnetic moments, and optical properties compared with isolated TM_m clusters. Furthermore, it is important to mention that TM particles can directly affect the chemical and physical properties of the environment, which can be used as a mechanism to tune the physical and chemical properties of different systems.

Experimental studies using spectroscopic ellipsometry measurements of Co clusters inside CNTs (Ref. 7) reveal a drastic change in the dielectric response,[7] which suggests that Co clusters can be used to tailor the optical properties of CNTs. High-resolution transmission electron microscopy (HRTEM) experiments have suggested that large Co particles inside CNTs have face-centered-cubic (fcc) structures,[10] instead of stable hexagonal-close-packed (hcp) structures;[11] i.e., the interaction of Co surface atoms with the inside CNT surfaces induces a structure phase change.

Recently, several theoretical studies have been reported for the encapsulation of TM atoms and clusters inside fullerenes and CNTs.[12–16] For example, Garg *et al.*,[14] using density functional theory (DFT), studied the encapsulation of $3d$ atoms inside small fullerenes, C_n ($n = 20-36$). They found that the C_n size plays an important role in the magnetic interactions, i.e., the system changes from ferromagnetic (FM) to antiferromagnetic (AFM). Ivanovskaya *et al.*,[12] employing tight-binding DFT calculations, found strong changes in the magnetic moments for Fe nanowires and clusters encapsulated inside CNTs.

Using DFT calculations, Javan *et al.*[15] found similar trends for Co_m ($m = 2-7$) inside C_{60} and C_{82}, i.e., large reduction in the magnetic moments, which was attributed to the strong Co-C hybridization. Furthermore, they found that $Co_m@C_{60}$ and $Co_m@C_{82}$ are energetically favorable for $m = 2-7$, except for $Co_7@C_{60}$. Javan *et al.*[16] also studied the encapsulation of Fe_m ($m = 2-7$) inside C_{60} and C_{80}. For both Fe_m and Co_m clusters in gas phase, Javan *et al.*[15,16] found highly symmetric TM configurations, which are substantially different from previous results,[17–22] i.e., previous DFT calculations found distorted structures for Fe_m and Co_m in gas phase. Furthermore, there is no explanation why the encapsulation energies for $Co_m@C_{60}$ and $Fe_m@C_{60}$ are so different, e.g., positive (unstable) even

for the diatomic Fe_2 molecule, while it is negative (stable) for Co_6 inside C_{60}.

Therefore, while the theoretical study of isolated TM_m clusters and NPs has been reported for a long time (see, e.g., Refs. 20–34), first-principles study of TM_m clusters inside C_n and CNTs is relatively recent, and hence, our understanding of the general trends that drive the stabilization of TM_m inside C_n and CNTs is far from satisfactory.

In this work, we will address the problem of encapsulation of magnetic TM_m (TM = Fe, Co, Ni; $m = 2-6$) clusters inside fullerene cages, C_n ($n = 60,70,80,90$) employing first-principles DFT calculations. It is well known that DFT within local or semilocal functionals cannot correctly describe the van der Waals interacitons, which are present for TM_m encapsulated inside fullerenes. In order to improve our description, we will employ an empirical correction to take into account the van der Waals interactions. Our aim is to obtain a better atomistic understanding of the effects of the encapsulation on the structure, stability, and magnetic properties of TM_m clusters. Furthermore, we expect that our results for $TM_m@C_n$ can also help to understand the encapsulation of TM_m clusters inside CNTs, as well as the role of the van der Waals interactions for encapsulation of TM_m clusters inside fullerenes.

II. THEORETICAL APPROACH AND COMPUTATIONAL DETAILS

Our calculations are based on spin-polarized DFT[35,36] within the generalized gradient approximation[37] (GGA) proposed by Perdew, Burke, and Ernzerhof (PBE),[38] and employing the all-electron projected augmented wave[39,40] (PAW) method as implemented in the Vienna *Ab initio* Simulation Package[41,42] (VASP). To improve the description of the van der Waals interactions, which might play an important role in the interaction of TM_m clusters inside fullerenes, we employed the empirical approach proposed by Grimme (DFT + D2),[43] which has a lower computational cost and it is currently implemented in VASP. In this approach the total energy, $E_{\mathrm{DFT+D2}}$, is obtained by the sum of the usual self-consistent DFT total energy with the van der Waals dispersion correction, E_{disp}, i.e.,

$$E_{\mathrm{DFT+D2}} = E_{\mathrm{DFT}} + E_{\mathrm{disp}}, \tag{1}$$

where

$$E_{\mathrm{disp}} = -\frac{s_6}{2}\sum_i \sum_j \frac{C_6^{ij}}{R_{ij}^6} f_{\mathrm{dmp}}(R_{ij}), \tag{2}$$

where i and j runs over the atoms in the unit cell. C_6^{ij} denotes the dispersion coefficient for atom pair ij ($C_6^{ij} = \sqrt{C_6^i C_6^j}$), s_6 is a global scaling factor that only depends on the exchange-correlation functional ($s_6 = 0.75$ for PBE), R_{ij} is the distance between the i and j atoms, and $f_{\mathrm{dmp}}(R_{ij})$ is a damped function to avoid near singularities for small distances. All the parameters employed in the DFT + D2 (PBE + D2 from now) framework are reported and discussed in Ref. 43.

For all PBE and PBE + D2 calculations, we employed a plane-wave cutoff energy of 400 eV within a cubic box of 22 Å and the Γ point for the Brillouin zone integration. The equilibrium geometries of all atomic configurations (fullerenes, TM_m, and $TM_m@C_n$) were obtained once the atomic forces on every atom are smaller than 0.025 eV/Å. The search for the lowest-energy configurations of TM_m clusters encapsulated inside C_n is a challenging problem due to the large number of local minimum configurations and the interaction of the TM atoms with the inside C_n surface.

In this work, we employed a sequence of steps to obtain a putative set of lowest-energy configurations for the $TM_m@C_n$ systems, which are summarized as follows: (i) Selection of spherical and ellipsoid (prolate) fullerene structures that obey the isolated pentagon rule, i.e., there are no adjacent pentagons,[44] which avoid strain induced by pentagon-pentagon contact. (ii) A large number of TM_m configurations were selected from previous studies for small TM_m clusters,[17–22] which include low coordination structures (open), high coordination structures (compact), and broken-symmetry structures. Furthermore, we selected several snapshots from first-principles simulated annealing (SA) simulations, which were initiated with a given structure with lower symmetry at high temperature (1000 K) and reduced to about 0 K in 10 picoseconds. (iii) The lowest-energy configurations obtained for TM_m in gas phase were placed at the center or near to the inside C_n surfaces to generate several initial $TM_m@C_n$ configurations. This procedure was repeated also for slightly higher energy TM_m configurations. (iv) Structural crossover was performed among the $TM_m@C_n$ configurations as suggested in Ref. 32, i.e., lowest-energy configurations identified for $Fe_m@C_n$ were considered as candidates for $Co_m@C_n$ and $Ni_m@C_n$ and vice versa. (v) Different spin-magnetic configurations were considered for TM_m and $TM_m@C_n$.

III. RESULTS

A. Fullerenes

Among a large number of C_n with different size, shape, and number of isomers,[44–46] we selected a set of C_n systems with four different sizes, namely, $n = 60,70,80,90$ (Fig. 1). There is one isomer for C_{60}, one for C_{70}, seven for C_{80}, and 46 for C_{90}, i.e., different cage shapes are available for particular C_n sizes ($n = 80,90$). To obtain a better understanding of the cage shape in the $TM_m@C_n$ properties, we selected two spherical fullerenes, C_{60}-I_h (Refs. 44,46–48 and C_{80}-I_h,[46,48,49] and two prolate fullerenes, C_{70}-D_{5h} (Refs. 44,46–48, and 50) and C_{90}-D_{5h}.[46,51] As a consequence of the Euler theorem, there are twelve pentagons in the C_{60}, C_{70}, C_{80}, and C_{90} cages, and the

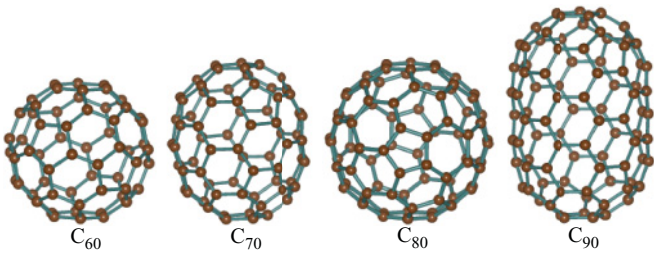

FIG. 1. (Color online) Atomic structures of the C_{60}-I_h, C_{70}-D_{5h}, C_{80}-I_h, and C_{90}-D_{5d} fullerenes optimized by DFT-PBE calculations.

number of hexagons close to the fullerene cages are 20, 25, 30, and 35, respectively. We would like to mention that C_{60}-I_h, C_{70}-D_{5h}, and C_{80}-I_h fullerenes have been widely observed experimentally,[44,45] while C_{90}-D_{5h} was only recently identified by single-crystal x-ray diffraction,[51] and has very interesting properties between fullerenes and CNTs.

The four selected C_n structures were optimized using the PBE and PBE + D2 functionals and employing symmetry constraint, i.e., I_h for C_{60} and C_{80}, and D_{5h} for C_{70} and C_{90}. We found that the PBE + D2 functional does not affect the geometry of the fullerenes. From our PBE results, we can estimate an average diameter for the spherical cages, namely, 7.10 Å for C_{60} and 8.13 Å for C_{80}, while two parameters are necessary for the prolate fullerenes, i.e., the equatorial radii (along the x and y axes) a, and the polar radius (along the z axis) c. For C_{70}, $a = 7.09$ Å and $c = 7.94$ Å, while for C_{90}, $a = 6.95$ Å and $c = 10.55$ Å. We estimated the cage volume ($V = \frac{4}{3}\pi a^2 c$, $a = c$ for spherical shape) as 1499, 1672, 2251, and 2135 Å^3 for C_{60}, C_{70}, C_{80}, and C_{90}, respectively, i.e., the cage volume increases from $C_{60} \rightarrow C_{70} \rightarrow C_{90} \rightarrow C_{80}$, which is expected to play an important role for TM_m encapsulation. The C-C bond lengths in C_n are from 1.39 to 1.45 Å, which is consistent with experimental results,[44,51] and substantially smaller than the TM-TM bond lengths,[11] which might affect the binding of the TM_m clusters to the inside C_n surfaces.

B. Isolated transition-metal clusters

For the isolated TM_m clusters, several configurations were calculated using PBE and PBE + D2 for each system, and there is not a significant difference between the PBE and PBE + D2 results. Thus, only the lowest-energy PBE TM_m structures are shown in Fig. 2. For the structural analysis of the TM_m clusters, we employed the effective coordination concept,[52,53] which yields the effective coordination number

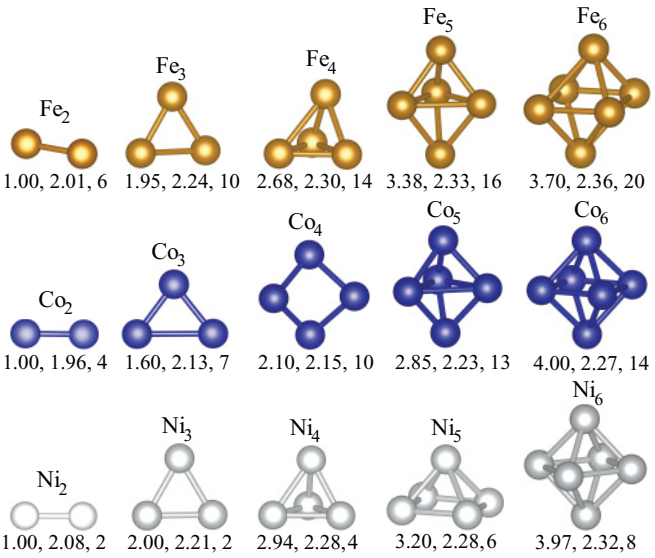

FIG. 2. (Color online) Lowest-energy DFT-PBE structures obtained for Fe_m, Co_m, and Ni_m for $m = 2-6$. The effective coordination numbers, the weighted average bond lengths (in Å), and the total magnetic moments (in μ_B) are given by the respective three numbers below every structure.

for all atoms, ECN_i, and the respective weighted bond length, d^i_{av}. In this work, ECN and d_{av} indicate the average results over all atoms in the TM_m cluster. This analysis has been employed in several TM cluster studies,[31,32,34,54] oxides,[55,56] and phase change materials.[53]

At their crystalline phases, Fe, Co, and Ni form compact structures, namely, body-centered cubic (bcc), hexagonal close-packed (hcp), and face-centered cubic (fcc), respectively;[11] however, the lowest-energy TM_m structures are not as compact as the well-known compact Lennard-Jones clusters (LJ).[57] For example, for LJ_m clusters, ECN = 1.0 (dimer), 2.0 (triangle), 3.0 (tetrahedral), 3.6 (trigonal bipyramid), and 4.0 (tetragonal bipyramid) for $m = 2,3,4,5,6$, respectively, however, for $m = 5$, we found ECN = 3.38 (Fe_5), 2.85 (Co_5), and 3.20 (Ni_5), while it is 3.36 for LJ_5 (Fig. 2). Furthermore, there is a large deviation for Co_4, i.e., ECN = 2.10, instead of 3.0 (LJ_4). Thus, there is a strong tendency of the magnetic TM_m clusters for lower symmetry structures, which helps to increase their energy stability due to splitting of the highest occupied states.

From the ECN results, Fig. 2, the Ni_m clusters are much more compact than the Fe_m and Co_m structures, and hence, we expect that this trend can affect the stability of the $TM_m@C_n$ systems, i.e., noncompact structures would occupy large volumes inside the fullerene cages. Except for TM_2, d_{av} increases slightly as a function of the TM_m size, e.g., 2.13 Å (Co_3) and 2.27 Å (Co_6). For TM_2, d_{av} has the smaller value, which is expected due to the lowest coordination (ECN = 1). Our lowest-energy structures are consistent with previous calculations based on DFT within semilocal functionals.[17–22]

The isolated Fe_m, Co_m, and Ni_m clusters are ferromagnetic as their respective bulk phases.[11] The total magnetic moments m_T of the TM_m clusters increase almost linearly as a function of cluster size, except small deviations, e.g., for Co_6 and Ni_2. As expected from results for the bulk phases,[11] m_T decreases from Fe to Ni clusters. For example, for Fe_6, Co_6, and Ni_6, $m_T = 3.33$, 2.33, and $1.33\mu_B$/atom, which is larger than for the bulk systems, i.e., $m_T = 2.21$, 1.62, and $0.64\mu_B$/atom, for Fe, Co, and Ni bulk, respectively. Our results and trends are in good agreement with previous results.[17–22]

C. TM_m at C_n

We calculated about 450 configurations for the $TM_m@C_n$ systems employing the PBE functional and following the procedure online in Sec. II with the aim to identify the best set of putative lowest-energy structures. All relaxed PBE geometries were reoptimized using the PBE + D2 functional.

1. Geometric parameters

We found only slight changes in the atomic structure of the $TM_m@C_n$ systems due to the van der Waals corrections, i.e., the changes in the ECN and d_{av} of the encapsulated TM_m clusters are between 2% and 5% for all cases. Thus, only the lowest PBE structures are shown in Fig. 3 along with the results for ECN and d_{av}, which we will use to identify the structural changes due to the encapsulation of the TM_m clusters inside C_n cages.

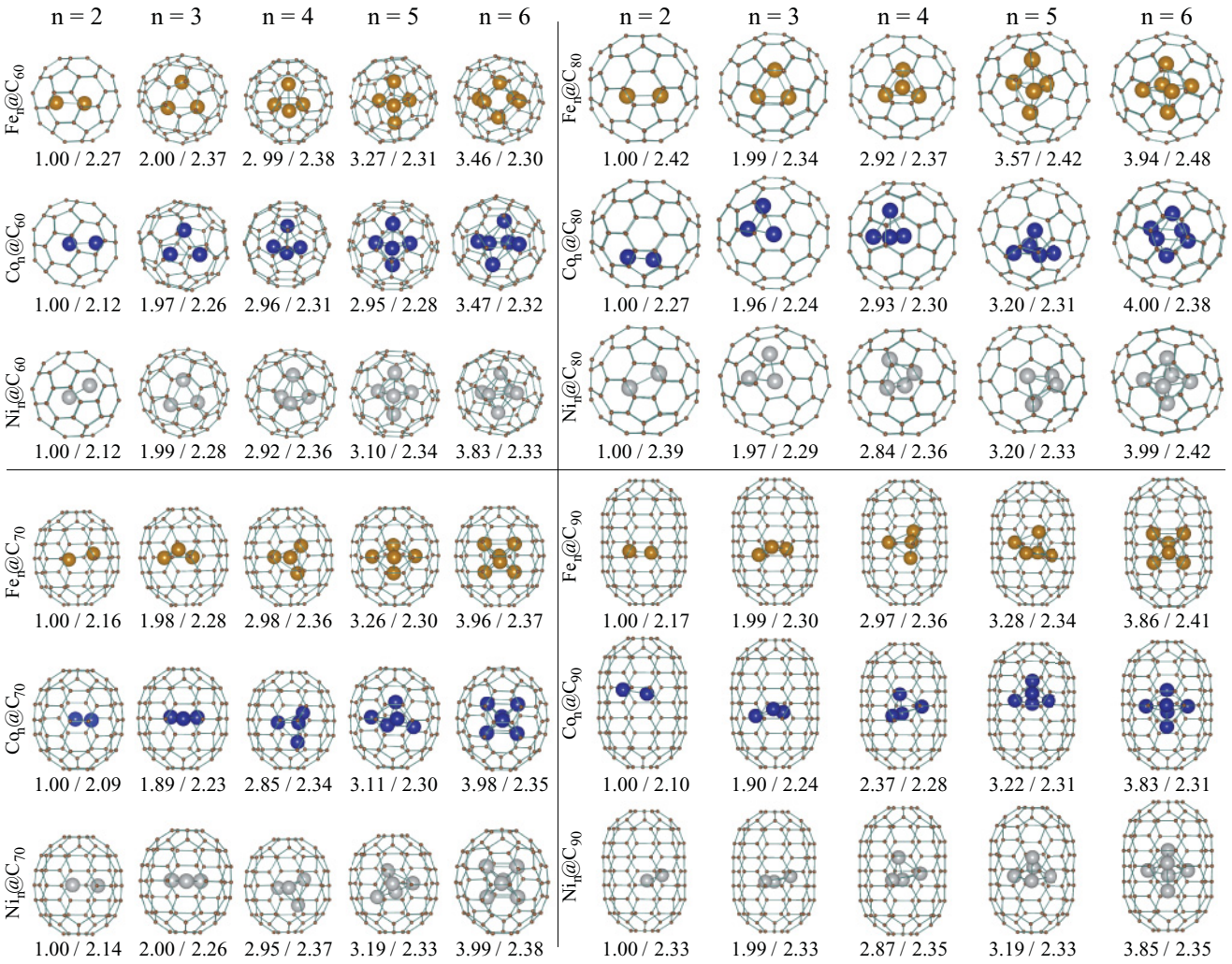

FIG. 3. (Color online) Atomic structures of the lowest-energy DFT-PBE configurations for the $TM_m@C_n$ systems (TM = Fe, Co, Ni; $m = 2,3,4,5,6$; $n = 60,70,80,90$). The numbers below the structures (ECN/d_{av}) indicate the average effective coordination number and average weighted bond lengths (in Å).

We found that the center of mass of the TM_m ($m = 2-4$) clusters displaces towards the inside C_n surface, which indicates an attractive interaction of the TM_m clusters by the inside C_n surface; however, large TM_m clusters ($m = 5$ and 6) are nearly located at the center of the cages due to the cluster and cage sizes. For all $TM_m@C_n$ systems, the smallest TM-C distances are in the range from 2.08 to 2.30 Å, which is typical for the bond lengths of Fe, Co, and Ni atoms with C atoms in metal complexes, e.g., 2.06 Å for Fe-C in $Fe(C_5Cl_5)_2$.[58] For most cases, the TM atoms bind to the center of the hexagonal or pentagonals, which maximizes the coordination number of the TM atoms.

From the results reported in Figs. 3 and 2, we can observe the following effects on TM_m. Except for Fe_5 and Fe_6 inside C_{60} and C_{70}, d_{av} increases for all clusters, e.g., changes from 2.01 Å for Fe_2 in gas-phase to 2.27, 2.16, 2.42, and 2.17 Å for Fe_2 inside C_{60}, C_{70}, C_{80}, and C_{90}, respectively. Similar changes can be observed for the other systems. The compression of the Fe_5 and Fe_6 bond lengths inside C_{60} and C_{70} can be explained by the small cage sizes of the C_{60} and C_{70} fullerenes as there is no similar compression for Fe_6 inside C_{80}. We would like to mention that the compression of the bond lengths occurs only for Fe_m clusters, which can be explained by the atomic radii differences between the TM atoms, i.e., Fe is slightly larger than Co and Ni, while Co and Ni have a similar atomic size. For example, using our calculated average weighted bond lengths for the bulk systems, the atomic radius ($d_{av}/2$) of Fe, Co, and Ni are 1.27, 1.25, and 1.24 Å, respectively, which is consistent with atomic radius reported in the literature, i.e., 1.32, 1.26, and 1.24 Å, for Fe, Co, and Ni, respectively.[11,59]

We noticed that most of the TM_m clusters increase their average effective coordination number inside fullerene cages, and hence, the TM_m clusters are more compact. For few cases, we found that the TM_m clusters change their lowest-energy structure upon the encapsulation, e.g., the Co_5 structure changes from trigonal bipyramid (isolated) to tetragonal upon the encapsulation in C_{70}, C_{80}, and C_{90} cages. The same effects happen also for Fe_4. Thus, this result indicates that not only the lowest-energy structures in gas phase should be considered

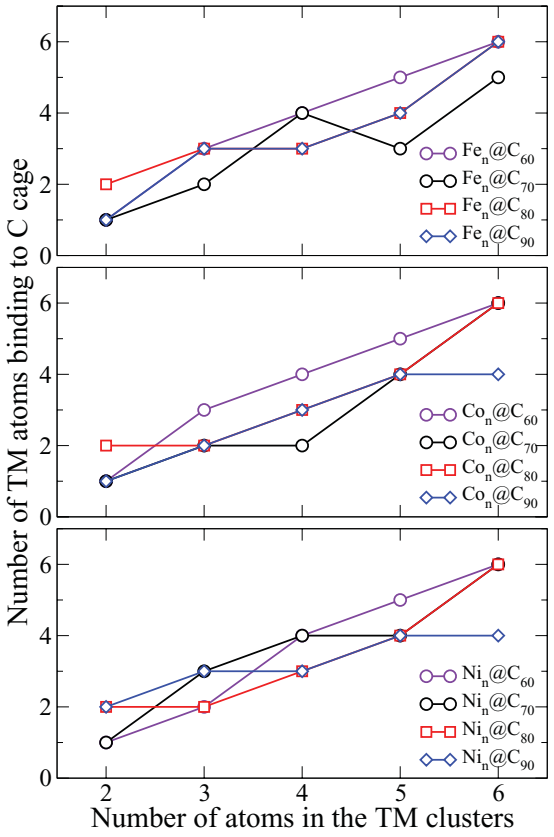

FIG. 4. (Color online) Number of transition-metal atoms binded directly to the inside fullerene surfaces of the lowest-energy $TM_m@C_n$ configurations (TM = Fe, Co, Ni; $m = 2,3,4,5,6$; $n = 60,70,80,90$).

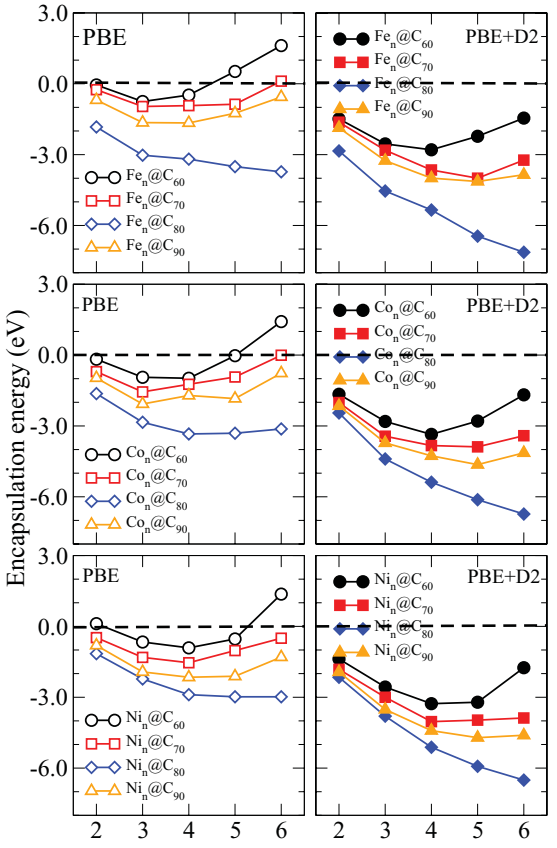

FIG. 5. (Color online) Encapsulation energy of the TM_m clusters inside C_n, $TM_m@C_n$ (TM = Fe, Co, Ni; $m = 2,3,4,5,6$; $n = 60,70,80,90$).

for encapsulation inside C_n cages. In Fig. 4, we summarize the number of TM atoms that binds directly to the inside fullerene surfaces as a function of the TM_m size. It can be seen that the number of atoms binded directly to the inside surfaces increases almost linearly with few deviations, which is expected to affect the encapsulation energy and magnetic properties.

2. *Encapsulation energy*

The encapsulation energy $E_{\rm enc}$, which measures the energy gain due to the encapsulation ($TM_m + C_n \rightarrow TM_m@C_n$), can be calculated by the following equation:

$$E_{\rm enc} = E_{\rm tot}^{{\rm TM}_m@{\rm C}_n} - \left(E_{\rm tot}^{{\rm C}_n} + E_{\rm tot}^{{\rm TM}_m}\right), \qquad (3)$$

where $E_{\rm tot}^{{\rm TM}_m@{\rm C}_n}$ is the total energy of the $TM_m@C_n$ system. $E_{\rm tot}^{{\rm C}_n}$ and $E_{\rm tot}^{{\rm TM}_m}$ are the total energies of the C_n and TM_m systems, respectively. A positive or negative value for $E_{\rm enc}$ indicates an energetically unfavorable or favorable system. Thus, it is important to obtain the range of values for m and n for which $E_{\rm enc}$ is negative. The PBE and PBE + D2 results for $E_{\rm enc}$ are shown in Fig. 5.

In contrast with the structural parameters (ECN, $d_{\rm av}$), the van der Waals correction strongly affects the encapsulation energy. For example, the dispersion correction to the PBE functional increases the stability of all systems by about a factor of 2, which is a substantial change; however, it is important to take into account that the magnitude of the change depends strongly on the magnitude of the C_6^{ij} parameters. Recent theoretical studies have suggested that Grimme's C_6^{ij} parameters in the PBE + D2 framework[43] might be overestimated,[60] which contributes to increase the van der Waals corrections to the binding energy. We would like to point out that both PBE and PBE + D2 functionals yield similar dependence of the encapsulation energy as a function of TM_m size for a particular C_n.

For a given TM_m size, the encapsulation energy gets more negative (increase stability) from $C_{60} \rightarrow C_{70} \rightarrow C_{90} \rightarrow C_{80}$. For example, for Co_2 (Co_6), $E_{\rm enc}^{\rm PBE} = -0.17$ (+1.42), −0.70 (−0.01), −0.97 (−0.77), and −1.63 eV (−3.13 eV) for C_{60}, C_{70}, C_{90}, and C_{80}, respectively. The same trend is also observed for the PBE + D2 results. We would expect this dependence for large TM_m clusters, but not for small diatomic molecules such as TM_2. We found that PBE (PBE + D2) yields a positive (negative) encapsulation energy for TM_6 inside C_{60}, and the stability of the $TM_6@C_n$ increases by increasing the C_n cage size, which is intuitively expected. For TM_2 inside C_n, we found that TM_2 adsorbs perpendicular to the hollow sites of the hexagonal rings for C_{60}, C_{70}, and C_{90}, i.e., only one TM atom directly binds to the C atoms; however, TM_2 adsorbs parallel to the surface inside C_{80}, and hence, two TM atoms bind directly to the surface, which increases the binding energy. Therefore, our results and analysis indicate that the curvature of the inside C_n surfaces affects directly the

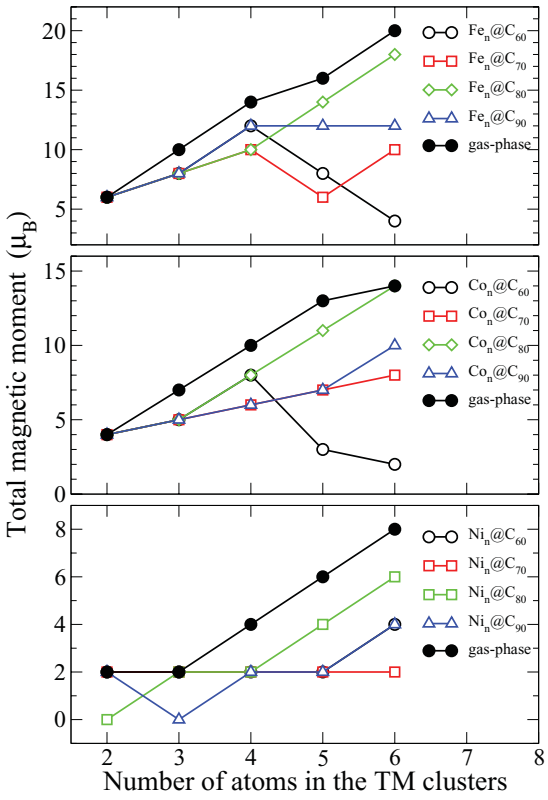

FIG. 6. (Color online) Total magnetic moments of the $TM_m@C_n$ systems (TM = Fe, Co, Ni; $m = 2,3,4,5,6$; $n = 60,70,80,90$). Results for TM_m in gas phase are also provided for comparison.

orientation of the TM_m clusters, and hence, the encapsulation energy.

For a particular C_n size and both PBE and PBE + D2 functionals, the encapsulation energy starts at a particular value for TM_2, and increasing the cluster TM_m size, the encapsulation energy turns more negative (increases stability) to reach a limit in which the stability decreases for large TM_m clusters. Thus, there is a minimum in the encapsulation energy of TM_m inside C_n as a function of the TM_m size for a particular value of n. For $TM_m@C_{80}$, our encapsulated TM_m clusters were not large enough to reach a minimum in the encapsulation energy; however, our results indicate that the same trends can be obtained. These results lead to the following question: Why is the stability larger for TM_3 and TM_4 than for TM_2? From our analysis, we found that the number of TM atoms that bind to the inside C_n surface plays a crucial role in increasing the stability of the $TM_m@C_n$ systems.

3. *Magnetic properties*

We found that the total magnetic moments are not affected by the van der Waals corrections, and hence, only the PBE results will be discussed below. The total magnetic moments of the lowest-energy $TM_m@C_n$ configurations are shown in Fig. 6 along with the results for the TM_m clusters in gas phase. The following trends can be observed: (i) Except for a few cases, the total magnetic moments decrease for encapsulated TM_m clusters compared with TM_m in gas phase, in particular, for

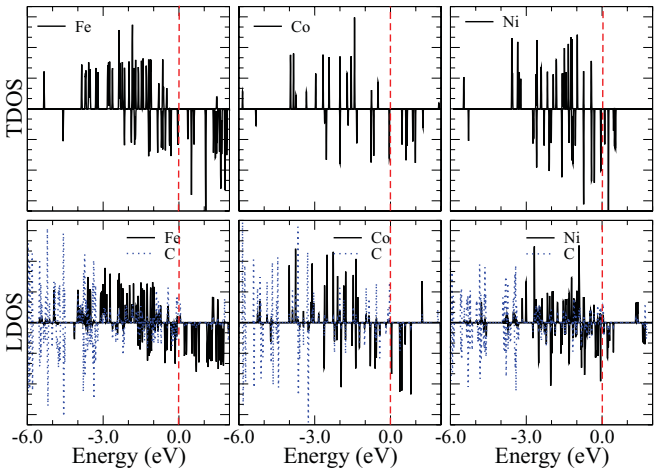

FIG. 7. (Color online) Total density of states (TDOS) of the TM_6 clusters. Local density of states (LDOS) of the TM and C atoms in the $TM_6@C_{80}$ system. The vertical red-dashed line (zero energy) indicates the energy of the highest occupied state.

large TM_m clusters inside small C_n cases, e.g., $m = 5,6$ inside C_{60}, C_{70}, and C_{90}. Therefore, our results indicate that the ratio between cluster and cage size plays a key role in the magnetic properties of encapsulated magnetic systems. (ii) For few $Ni_m@C_n$ systems, e.g., $Ni_3@C_{90}$, we found that the magnetic solutions change from ferromagnetic to antiferromagnetic or ferrimagnetic phases. (iii) For most of the systems, we observed a large number of atomic configurations with similar total energies, i.e., differences smaller than 5.0 meV per TM atom, and slightly different magnetic moments. This result indicates that at real experimental conditions one of the magnetic configurations might be more favorable or a wide range of magnetic configurations might exist, and experimental techniques might access only the average results.

4. *Density of states*

To obtain a better understanding of the electronic properties of the $TM_m@C_n$ systems, we calculated the total and local density of states (TDOS, LDOS). The PBE and PBE + D2 functionals yield very similar TDOS and LDOS as both functionals yield very similar structural geometries for TM_m and $TM_m@C_n$. For TM_6 and $TM_6@C_{80}$, the PBE results are shown in Fig. 7. As expected, the TDOS of the TM_6 clusters are dominated by the d states, which interact with the C p states and give rise to the hybridization of the p-d states, however, it is not simple to identify clear trends in the TDOS and LDOS of the $TM_m@C_n$ systems. To improve our analysis, we calculate the center of gravity of the occupied d states, C_g^d (majority and minority spins) for isolated and encapsulated TM_m clusters. The results are shown in Fig. 8.

For the isolated TM_m clusters, we found that C_g^d (majority spin) $< C_g^d$ (minority spin), i.e., the center of gravity of the minority spin is closer to the highest occupied d state. As expected, C_g^d changes with the number of TM atoms in the TM_m clusters, e.g., for Fe_m, the changes occur mainly for the minority spin, while C_g^d (majority spin) is almost constant for $m = 2-7$. However, it is in contrast with the results obtained

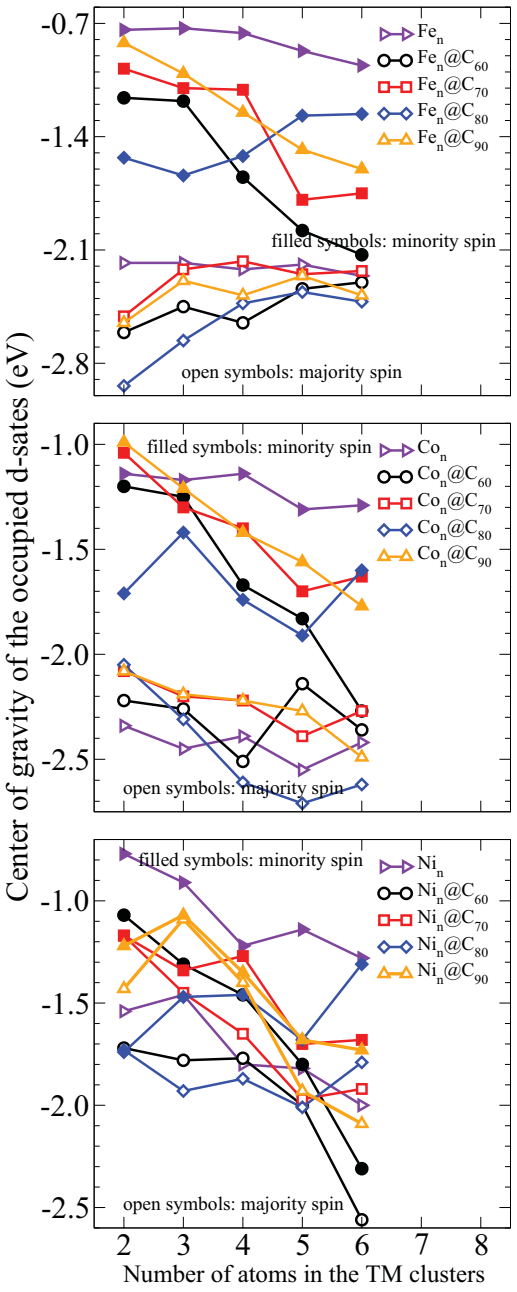

FIG. 8. (Color online) Center of gravity of the occupied d states of the TM atoms encapsulated inside the C_n. Zero energy indicates the highest occupied state in the $TM_m@C_n$ system.

for Co_m and Ni_m, i.e., the center of gravity of both majority and minority spins are strongly affected by the size of the TM_m clusters.

We found large changes in the center of gravity of the d states upon the encapsulation, which is expected due to the strong interaction with the inside C_n surfaces. The largest changes in the center of gravity occur for $TM_m@C_{60}$, in particular, for large clusters, TM_6, which is expected due to the large size of the TM_6 clusters and small internal volume of the C_{60} cage that yields a nearly zero encapsulation energy for $Fe_6@C_{60}$. We noticed that the orientation of the TM_m clusters also affects the magnitude of the shift. For example, for $TM_2@C_n$, the largest C_g^d shift occurs for $Fe_2@C_{80}$ due to the parallel orientation of Fe_2 with respect to the inside C_{80} surface. There is no clear trend in the magnitude of the shift of the center of gravity and the magnitude of the encapsulation energy. Similar results are observed for $Co_m@C_n$ and $Ni_m@C_n$, however, with smaller magnitudes. For almost all configurations, the center of gravity of the d states shifts down upon the encapsulation.

IV. CONCLUSIONS

In this work, we performed PBE and PBE + D2 (empirical Grimme's correction for van der Waals interactions) calculations for $TM_m@C_n$ (TM = Fe, Co, Ni, Co; $m = 2-6$; $n = 60,70,80,90$). From a large number of calculations, we obtained a set of putative lowest-energy configurations for $TM_m@C_n$, which were used to calculate the encapsulation energy, total magnetic moments, density of states, and center of gravity of the occupied d states. From our results and analysis, the following trends were identified.

The van der Waals corrections strongly affect the encapsulation energy, while the structural parameters and magnetic moments are affected slightly. We would like to point out that the dispersion correction to the PBE functional increases the stability of all the $TM_m@C_n$ systems by about a factor of 2, which might be related with the overestimation of the C_6^{ij} parameters[60] in Grimme's PBE + D2 framework.[43] Thus, our results suggest that the correct values of the encapsulation energies depend on the correct treatment of the correlation effects, which might require theoretical approaches such as the quantum Monte Carlo approach.

The center of mass of the TM_m clusters is displaced towards the inside C_n surfaces, except for large TM_m clusters ($m = 5-6$), which are almost located at the center of the C_n cages due to the cluster and cage sizes. The effective coordination number and average bond lengths of TM_m clusters increase inside fullerenes. For particular cases, e.g., Co_4 and Fe_4, the encapsulation changes the lowest-energy structure compared with the gas phase, i.e., the lowest-energy configuration depends on the environment. The total magnetic moments of the TM_m clusters inside fullerenes decrease, in general, compared with TM_m in gas phase, in particular, for large clusters inside small C_n cages.

We identified three key parameters that play an important role in the sign and magnitude of the encapsulation energy: (i) The TM_m size and volume of the C_n cage. (ii) The curvature of the inside C_n surfaces. (iii) The number of TM atoms that bind directly to the inside C_n surface. Therefore, these three terms play a crucial role in the minimum of the encapsulation energy curve as a function of TM_m cluster size for a particular C_n. Thus, we believe that our conclusions can help to improve the understanding of encapsulation of TM clusters inside fullerenes.

ACKNOWLEDGMENTS

We thank São Paulo Science Foundation (FAPESP) for support. We thank Maurício J. Piotrowski and Anderson S. Chaves for reading the manuscript.

*pltereshchuk@mail.ru
†Corresponding author: dasilva_juarez@yahoo.com

[1] J. L. F. Da Silva, M. V. Ganduglia-Pirovano, J. Sauer, V. Bayer, and G. Kresse, Phys. Rev. B **75**, 045121 (2007).
[2] J. L. F. Da Silva, M. V. Ganduglia-Pirovano, and J. Sauer, Phys. Rev. B **76**, 125117 (2007).
[3] F. Vila, J. J. Rehr, J. Kas, R. G. Nuzzo, and A. I. Frenkel, Phys. Rev. B **78**, 121404(R) (2008).
[4] S. Vajda, M. J. Pellin, J. P. Greeley, C. L. Marshall, L. A. Curtiss, G. A. Ballentine, J. W. Elam, S. Catillon-Mucherie, P. C. Redfern, F. Mehmood, and P. Zapol, Nat. Mater. **8**, 213 (2009).
[5] A. Wijaya, S. B. Schaffer, I. G. Pallares, and K. Hamad-Schifferli, ACS Nano **3**, 80 (2009).
[6] X. Pan, Z. Fan, W. Chen, Y. Ding, H. Luo, and X. Bao, Nat. Mater. **6**, 507 (2007).
[7] C. Soldano, F. Rossella, V. Bellani, S. Giudicatti, and S. Kar, ACS Nano **4**, 6573 (2010).
[8] R. Jurgons, C. Seliger, A. Hilpert, L. Trahms, S. Odenbach, and C. Alexiou, J. Phys.: Condens. Matter **18**, S2893 (2006).
[9] K. Braun, L. Dunsch, R. Pipkorn, M. Bock, T. Baeuerle, S. Yang, W. Waldeck, and M. Wiessler, Int. J. Med. Sci. **7**, 136 (2010).
[10] X. Ma, Y. Cai, N. Lun, Q. Ao, S. Li, F. Li, and S. Wen, Mater. Lett. **57**, 2879 (2003).
[11] C. Kittel, *Introduction to Solid State Physics, 7th ed.* (Wiley, New York, 1996).
[12] V. V. Ivanovskaya, C. Köhler, and G. Seifert, Phys. Rev. B **75**, 075410 (2007).
[13] P. F. Weck, E. Kim, K. R. Czerwinski, and D. Tomanek, Phys. Rev. B **81**, 125448 (2010).
[14] I. Garg, H. Sharma, N. Kapila, K. Dharamvir, and V. K. Jindal, Nanoscale **3**, 217 (2011).
[15] M. B. Javan, N. Tajabor, M. Rezaee-Roknabadi, and M. Behdani, Appl. Surf. Sci. **257**, 7586 (2011).
[16] M. B. Javan and N. Tajabor, J. Magn. Magn. Mater. **324**, 52 (2012).
[17] P. Ballone and R. O. Jones, Chem. Phys. Lett. **233**, 632 (1995).
[18] M. Castro, C. Jamorski, and D. R. Salahub, Chem. Phys. Lett. **271**, 133 (1997).
[19] Q. M. Ma, Y. Liu, Z. Xie, and J. Wang, J. Phys.: Conf. Ser. **29**, 163 (2006).
[20] S. Datta, M. Kabir, S. Ganguly, B. Sanyal, T. Saha-Dasgupta, and A. Mookerjee, Phys. Rev. B **76**, 014429 (2007).
[21] S. Yu, S. Chen, W. Zhanga, L. Yu, and Y. Yin, Chem. Phys. Lett. **446**, 217 (2007).
[22] P. L. Tereshchuk, Comput. Mater. Sci. **50**, 991 (2011).
[23] R. Fournier, J. Chem. Phys. **115**, 2165 (2001).
[24] F. Aguilera-Granja, J. L. Rodríguez-López, K. Michaelian, E. O. Berlanga-Ramírez, and A. Vega, Phys. Rev. B **66**, 224410 (2002).
[25] S.-R. Liu, H.-J. Zhai, and L.-S. Wang, Phys. Rev. B **65**, 113401 (2002).
[26] G. Rollmann and P. Entel, Comput. Lett. **1**, 288 (2004).
[27] Q.-M. Ma, Z. Xi, J. Wang, Y. Liu, and Y.-C. Li, Solid State Commun. **142**, 114 (2007).
[28] S. Rives, A. Catherinot, F. Dumas-Bouchiat, C. Champeaux, A. Videcoq, and R. Ferrando, Phys. Rev. B **77**, 085407 (2008).
[29] Y. Sun, M. Zhang, and R. Fournier, Phys. Rev. B **77**, 075435 (2008).
[30] F. Aguilera-Granja, L. C. Balbás, and A. Vega, J. Phys. Chem. A **113**, 13483 (2009).
[31] J. L. F. Da Silva, H. G. Kim, M. J. Piotrowski, M. J. Prieto, and G. Tremiliosi-Filho, Phys. Rev. B **82**, 205424 (2010).
[32] M. J. Piotrowski, P. Piquini, and J. L. F. Da Silva, Phys. Rev. B **81**, 155446 (2010).
[33] P. Błonski and J. Hafner, J. Phys.: Condens. Matter **23**, 136001 (2011).
[34] M. J. Piotrowski, P. Piquini, M. M. Odashima, and J. L. F. Da Silva, J. Chem. Phys. **134**, 134105 (2011).
[35] P. Hohenberg and W. Kohn, Phys. Rev. **136**, B864 (1964).
[36] W. Kohn and L. J. Sham, Phys. Rev. **140**, A1133 (1965).
[37] J. P. Perdew, J. A. Chevary, S. H. Vosko, K. A. Jackson, M. R. Pederson, D. J. Singh, and C. Fiolhais, Phys. Rev. B **46**, 6671 (1992).
[38] J. P. Perdew, K. Burke, and M. Ernzerhof, Phys. Rev. Lett. **77**, 3865 (1996).
[39] P. E. Blöchl, Phys. Rev. B **50**, 17953 (1994).
[40] G. Kresse and D. Joubert, Phys. Rev. B **59**, 1758 (1999).
[41] G. Kresse and J. Hafner, Phys. Rev. B **48**, 13115 (1993).
[42] G. Kresse and J. Furthmüller, Phys. Rev. B **54**, 11169 (1996).
[43] S. Grimme, J. Comp. Chem. **27**, 1787 (2006).
[44] P. W. Fowler and D. E. Manolopoulos, *An Atlas of Fullerenes* (Clarendom, Oxford, 1995).
[45] M. S. Dresselhaus, G. Dresselhaus, and P. C. Eklund, *Science of Fullerenes and Carbon Nanotubes* (Academic Press, San Diego, 1996), p. 17.
[46] A. Hirsch and M. Brettreich, *Fullerenes: Chemistry and Reactions* (Wiley-CVH Verlag GmbH & Co. KGaA, Weinheim, 2005).
[47] W. Krätschmer, L. D. Lamb, K. Fostiropoulos, and D. R. Huffman, Nature (London) **347**, 354 (1990).
[48] N. Kurita, K. Kobayashi, H. Kumahora, K. Tago, and K. Ozawa, Chem. Phys. Lett. **188**, 181 (1992).
[49] M.-L. Sun, Z. Slanina, S.-L. Lee, F. Uhlík, and L. Adamowicz, Chem. Phys. Lett. **246**, 66 (1995).
[50] V. Schettino, M. Pagliai, and G. Cardini, J. Phys. Chem. A **106**, 1815 (2002).
[51] H. Yang, C. M. Beavers, Z. Wang, A. Jiang, Z. Liu, H. Jin, B. Q. Mercado, M. M. Olmstead, and A. L. Balch, Angew. Chem., Int. Ed. **49**, 886 (2010).
[52] R. Hoppe, Z. Kristallogr. **150**, 23 (1979).
[53] J. L. F. Da Silva, J. Appl. Phys. **109**, 023502 (2011).
[54] M. J. Piotrowski, P. Piquini, L. Cândido, and J. L. F. Da Silva, Phys. Chem. Chem. Phys. **13**, 17242 (2011).
[55] J. L. F. Da Silva, A. Walsh, and S.-H. Wei, Phys. Rev. B **80**, 214118 (2009).
[56] A. Walsh, J. L. F. Da Silva, and S.-H. Wei, Chem. Mater. **21**, 5119 (2009).
[57] D. J. Wales and J. P. K. Doye, J. Phys. Chem. A **101**, 5111 (1997).
[58] L. Phillips, M. K. Cooper, A. Haaland, S. Samdal, N. I. Girichevad, and G. V. Giricheve, Dalton Trans. **39**, 4631 (2010).
[59] B. Cordero, V. Gómez, A. E. Platero-Prats, M. Revés, J. Echeverría, E. Cremades, F. Barragán, and S. Alvarez, Dalton Trans. 2832 (2008).
[60] K. Tonigold and A. Groß, J. Chem. Phys. **132**, 224701 (2010).